Optical-magnetism-induced transparency in a metamaterial

Ling Qin, Kun Zhang, Ru-Wen Peng, Xiang Xiong, Wei Zhang, Xian-Rong Huang, and Mu Wang

Phys. Rev. B **87**, 125136 — Published 22 March 2013

DOI: 10.1103/PhysRevB.87.125136

Optical-Magnetism-Induced Transparency in a Metamaterial

Ling Qin[1], Kun Zhang[1], Ru-Wen Peng[1,*], Xiang Xiong[1], Wei Zhang[1],

Xian-Rong Huang[2], and Mu Wang[1,*]

1) National Laboratory of Solid State Microstructures and Department of Physics, Nanjing University, Nanjing 210093, China

2) Advanced Photon Source, Argonne National Laboratory, Argonne, Illinois 60439, USA

Abstract

In this work, we theoretically demonstrate that electromagnetic transparency can be induced by optical magnetism in a metamaterial, which is composed of meta-molecules. Each meta-molecule consists of a metallic split-ring resonator (SRR) as one bright meta-atom (which is optically magnetic) and also a cut-wire pair (CWP) as one dark meta-atom (which is optically nonmagnetic). It is found that magnetic resonances occur at optical frequencies due to the local magnetic interaction between "bright" meta-atoms and "dark" meta-atoms, thereafter, a transparency window emerges upon the original absorption background. The phenomenon is similar to the electromagnetically induced transparency (EIT) in atomic three-level systems, and a microscopic picture is given to compare it with the EIT. Furthermore, low loss and slow light in this metamaterial have also been verified. The investigations may achieve potential applications on integrated optical circuits.

PACS numbers: 78.20.Ci, 42.25.Bs, 78.67.Pt

Keywords: Metamaterials; Optical magnetism; Electromagnetic transparency

* Electronic address: rwpeng@nju.edu.cn; muwang@nju.edu.cn

I. Introduction

It is well known that solids are composed of atoms and properties of solids rely on both the type and the arrangement of atoms. Some significant electromagnetic features, such as negative refraction introduced initially by Veslargo [1] in 1968, have been theoretically investigated but hard to be experimentally realized in natural materials for a long period. Interestingly based on similar relationship of solids and atoms, Pendry and his coauthors proposed metamaterials in 1999 [2], which consist of artificial "atoms", *i.e.* meta-atom, with particular permittivity and permeability via deliberately designing metallic and dielectric microstructures. It has been shown that metamaterials [2-4] provide a new paradigm to control the electromagnetic properties of materials beyond the nature. For example, metamaterials offer the possibilities for optical magnetism [5-7], superlenses [8,9], negative index of refraction [10,11], invisibility cloaking [12,13] and many other fascinating phenomena and applications beyond the reach of natural materials.

Now that metamaterials are constructed by meta-atoms, some physical phenomena in the naturally atomic systems can be re-exhibited in some artificially "atomic" systems. For instance, similar effect of electromagnetically induced transparency (EIT) has been achieved in the metamaterials in recent years [14-25]. As we know, EIT is a quantum interference phenomenon in atomic systems. It usually takes place in three-level atomic systems. The quantum interference effect induces a "transparency window" within the zone of resonance absorption, which is accompanied simultaneously by extremely slow group velocity of the referenced light wave. Recently, the group velocity of a light pulse can be reduced even to only 17m/s [26]. Due to the fact that the EIT in the atomic systems was observed usually at extremely low temperature, the technique applications of EIT become very limited. However, EIT-like behavior in metamaterials can be achieved at more convenient ways. For example, Zhang *et al.* [14] theoretically demonstrated that by making a plasmonic "molecule", which consists of a radiative element ("bright atom") and a subradiant element ("dark atom"), EIT-like behavior can be achieved in this metamaterial. Recently the EIT-like phenomena in metamaterials have been experimentally observed at

microwave[15], terahertz[16,17], near-infrared[19], and optical frequencies[20,21], all of which appear at room temperature. However, most of these works rely on the electric interaction between different elements in the materials, only few works are related to the magnetic interaction [22]. Physically, the magnetic interaction is much weaker than the electric interaction, therefore, it is more difficult to realize EIT in optically magnetic metamaterials.

In this work, we theoretically demonstrate that electromagnetic transparency can be induced by optical magnetism in a metamaterial, which is composed of meta-molecules (without any magnetic elements). Each meta-molecule consists of a metallic split-ring resonator (SRR) as "bright atom" and also a metallic cut-wire pair (CWP) as "dark atom", where the former is optically magnetic but the latter is optically nonmagnetic. It is well known that the metamaterial with a SRR as its building block has an optically magnetic resonance at specific frequency; and the metamaterial with a CWP as its building block has no magnetic resonance when the electric field of the incident light perpendicular to the wires. However, when we compose these two building blocks as one meta-molecule, the local magnetic fields between "bright" meta-atoms and "dark" meta-atoms may have destructive interference, thereafter, a transparency window emerges upon the original absorption background. This phenomenon is similar to the EIT in a three-level atomic system.

The manuscript is organized as following. We start from a general description of the EIT in a metamaterial, which is induced by optical magnetism in Sec. II. Then we show that "bright" meta-atom is optically magnetic and "dark" meta-atom is optically nonmagnetic. By combining these two meta-atoms, an optically magnetic meta-molecule is achieved in Sec. III. Then in Sec. IV, the EIT-like behavior in this optically magnetic metamaterial has been demonstrated by transmission spectra and spatial distribution of electromagnetic fields. Low loss and slow light in this metamaterial have also been verified. Further, an analog of microscopic picture for EIT in a metamaterial and that in an atomic three-level system is presented in Sec. V. Finally, a summary is given in Sec. VI.

II. A general description of EIT-like phenomenon induced by optical magnetism

First, we consider a system with two magnetic dipoles $\boldsymbol{M_1}$ and $\boldsymbol{M_2}$. Suppose that the coupling between the magnetic dipole $\boldsymbol{M_1}$ and the external electromagnetic field is strong enough, but the coupling between the magnetic dipole $\boldsymbol{M_2}$ and the external electromagnetic field can be negligible. With this assumption, the dynamic equations of the system can be written as

$$\begin{cases} \dfrac{d^2M_1(t)}{dt^2}+\gamma_1\dfrac{dM_1(t)}{dt}+\omega_0^2M_1(t)-\Omega^2M_2(t)=H_0(t) \\ \dfrac{d^2M_2(t)}{dt^2}+\gamma_2\dfrac{dM_2(t)}{dt}+\omega_0^2M_2(t)-\Omega^2M_1(t)=0 \end{cases}, \tag{1}$$

where γ_1 and γ_2 are the damping rate of $\boldsymbol{M_1}$ and $\boldsymbol{M_2}$, respectively, ω_0 is the resonant frequency of these two magnetic dipoles, and Ω is the coupling coefficient between the two magnetic dipoles. Considering an external field with frequency ω, then we have

$$\begin{cases} H_0(t)=H_0e^{-i\omega t} \\ M_1(t)=M_1e^{-i\omega t} \\ M_2(t)=M_2e^{-i\omega t} \end{cases}.$$

Thereafter, the magnetic dipole $\boldsymbol{M_1}$ follows

$$M_1=\frac{\omega_0^2-\omega^2-i\gamma_2\omega}{(\omega_0^2-\omega^2-i\gamma_1\omega)(\omega_0^2-\omega^2-i\gamma_2\omega)-\Omega^4}H_0. \tag{2}$$

Under the second-order approximation, the magnetic susceptibility in the system can be written as

$$\chi_H=\frac{M_1}{H_0}\cong(\omega^2-\omega_0^2)\frac{(\Omega^4-\gamma_2^2\omega^2)}{(\Omega^4+\gamma_1\gamma_2\omega^2)^2}+i\frac{\gamma_2\omega}{\Omega^4+\gamma_1\gamma_2\omega^2}. \tag{3}$$

According to Eq.(3), it is obvious that the real part of the magnetic susceptibility equals to

zero if $\omega = \omega_0$; and the imaginary part of the magnetic susceptibility equals to zero in the ideal case of $\gamma_2 = 0$. Therefore, Equation (3) indicates that a transparent window exists around the resonant frequency (ω_0) in the system with two magnetic dipoles.

III. Optically magnetic meta-molecules

It is well known that at optical frequencies, magnetic permeability (μ) for natural occurring materials is close to its value in free space. This is because the magnetic-field component of light couples to atoms much more weakly than the electric-field component does. However, this weak-coupling effect in naturally atomic systems can be overcome by using meta-atoms and metamaterials. As Pendry *et al.* [2] suggested initially, high-frequency magnetism can be achieved by exploiting the inductive response from non-magnetic structured materials. This idea was successfully implemented by using arrays of copper split-ring resonators (SRRs) that generated a magnetic response at frequencies up to 100THz [6]. Considering that a SRR shows a strong local magnetic resonance when the magnetic field of the incident light perpendicular to the SRR plane, it can serve as an optically magnetic "bright atom". The resonance frequency can be readily tuned by varying its spatial dimension. Because of the strong magnetic resonance, the local magnetic field near the magnetic "bright atom" can be dramatically enhanced. In the following text, the numerical calculation is carried out by using the commercial finite difference time domain (FDTD) software package (CST Microwave Studio). The permittivity of gold in the infrared regime was calculated by Drude model, *i.e.*, $\varepsilon(\omega) = 1 - \omega_p^2 / (\omega^2 + i\omega_\tau \omega)$, where ω_p is the plasmon frequency and ω_τ is the damping constant. For gold, the characteristic frequency were taken as $\omega_p = 1.37 \times 10^4 \text{THz}$, and $\omega_\tau = 40.84 \text{THz}$. In the simulation, the plane-wave source is put at the location of 1μm away from the sample. Non-uniform meshes are defined and the minimum mesh is about 0.002μm. The boundary conditions are set as following: along x direction the boundary is perfectly matched layer (PML);

while along both y and z directions the periodic boundary conditions are applied.

Figure 1(a) illustrates the geometry of a SRR under the polarized incident light. As shown in Fig. 1(c), the amplitudes for both electric fields and magnetic fields in the center of the SRR have been calculated as a function of frequency. It is evident that there exists a purely magnetic resonance around ω_0=192THz in the SRR. Meanwhile for a cut-wire pair (CWP), it consists of two parallel metal strips with a separation (as shown in Fig. 1(b)). When the polarized light illuminates the CWP, the local electric-field and magnetic-field amplitudes in the center of the CWP are illustrated in Fig. 1(d). We can find that an extremely weak magnetic resonance appears around ω_0=192THz, and no electric resonance is observed. Actually the resonance frequency can be tuned by the geometric parameters of the CWP. It is found that the resonance frequency of CWP will have a red shift if we increase the size of metal strips (i.e., u) and the separation of two strips (i.e., w) in Fig. 1(b). Simply by changing these two parameters, we can easily let the resonance in the CWP appear at the same frequency (ω_0) of that in the SRR. In order to evaluate these magnetic resonances, the factor of resonant amplitude is defined as

$$I = \frac{H_{\max} - H_{\min}}{H_{\max} + H_{\min}}, \qquad (4)$$

where H_{max} and H_{min} are the maximum and the minimum of the magnetic field intensities, respectively. Thereafter, the factor of resonant amplitude is $I \cong 0.5$ in the present SRR, but $I \cong 0.003$ in the present CWP. Physically in the SRR, the magnetic resonance originates from the magnetic dipole [6]; while in the CWP, the magnetic resonance comes from a pair of surface currents, one of which goes along **x** direction but the other goes along **–x** direction. These surface currents are induced by the magnetic field, but the magnetic field in CWP is much smaller than electric field in the incident light, so the resonance in the CWP becomes much weaker. Due to the fact that the magnetic resonance in the SRR is much stronger than that in the CWP, the SRR can act as a magnetic "bright atom" and the CWP can serve as a magnetic "dark atom".

By putting a "bright atom" and a "dark atom" together, a magnetic meta-molecule is

achieved as shown in Fig. 2(a). When the polarized incident light illuminates this meta-molecule, we have calculated the magnetic field amplitude versus frequency in the center of the system (Fig. 2(b)). As shown in Fig. 2(b), two magnetic resonances have been observed, which actually corresponds to a symmetric mode (ω_-) and an antisymmetric mode (ω_+), respectively. The microscopic physical process is as following. When the light shines this meta-molecule (the magnetic field of the incident light is perpendicular to the SRR plane), the "bright atom" (SRR) is excited around ω_0 =192THz and the local magnetic field around the SRR becomes very strong. Further, this strong local magnetic field near the bright atom enhances the magnetic resonance of the "dark atom" (CWP). Then there appear two magnetic dipoles, and the interaction between these two dipoles leads to the split of the original mode. Therefore, we observed two different magnetic modes (as shown in Fig. 2(b)): a symmetric mode at ω_- =178THz and an antisymmetric mode at ω_+ =205THz. Actually for the mode ω_- =178THz, the magnetic field in SRR has the same direction as that in CWP (to see Fig.2(c)), therefore, this mode is a symmetric mode; while for ω_+ =205THz, the magnetic field in SRR has the opposite direction as that in CWP (to see Fig.2(d)), therefore, this mode belongs to an antisymmetric mode.

IV. EIT-like effect in the optically magnetic metamaterial

Now we construct an optically magnetic metamaterial, where the meta-molecule is used as a building block and arranged in series to form a square lattice (schematically shown in Fig. 3(a)). For example, the magnetic meta-molecules (described in Sec. III) are arranged periodically with a spacing of 1μm in the *y*-*z* plane. We have calculated the transmission coefficients (*T*) of this metamaterial based on the definition of $T(\omega) = \frac{|E(\omega)|}{|E_0(\omega)|}$, where $E_0(\omega)$ and $E(\omega)$ are the incident and the transmitted electric fields, respectively. As shown in Fig. 3(b), two transmission dips are observed at ω_L =184THz and ω_H =201THz, respectively. By calculating the spatial distribution of magnetic fields in the metamaterial at these frequencies, we find that these two dips

actually correspond to the symmetric mode and the antisymmetric mode, respectively. For the case of the symmetric mode (ω_L), all the magnetic dipoles are in the same direction as shown in Fig. 3(d); while for the case of the antisymmetric mode (ω_H), two magnetic dipoles in each building block are in opposite directions as shown in Fig. 3(e). Besides, we have also retrieved the effective permeability of the based on Ref. [27]. As illustrated in Fig. 3(c), two Lorentz resonances appear at ω_L=184THz and ω_H=201THz, which correspond to the symmetric and the antisymmetric modes, respectively. Physically, because of these two strong resonances of the effective permeability (as shown in Fig.3(c)), the electromagnetic energies of the resonant modes (ω_L and ω_H) are confined mainly in bright meta-atoms (*i.e.*, SRR), which finally lead to two sharp dips in their transmission spectra (as shown in Fig.3(b)).

More interestingly, a transmission window around ω_{EIT}=191THz appears between two transmission dips (as shown in Fig. 3(b)), and it exists on the original absorption background. The EIT-like phenomenon originates from the fact that the "bright" meta-atom (*i.e.*, SRR) is excited by two different approaches: one is directly by the incident light, and the other is by the magnetic field of the excited "dark" meta-atom (*i.e.*, CWP). The destructive interference between these two approaches suppresses the excitation of the "bright" meta-atom (*i.e.*, SRR) and thereafter generates the transparent window. As shown in Fig. 3(f), around the frequency of ω_{EIT}=191THz, the magnetic field is mainly concentrated on the "dark atom" (*i.e.*, CWP), while the magnetic field becomes very weak around the "bright atom" (*i.e.*, SRR). Therefore, the effect in this optically magnetic metamaterial can be considered as an analogy of the EIT in atomic three-level systems.

Now that destructive interference occurs at the transparent window around ω_{EIT}, we can expect that magnetic susceptibility of this metameterial should approach zero at corresponding frequencies. Figure 4(a) shows the magnetic susceptibility of the metameterial. It is obvious that near the transparency window, the real and imagine parts of the magnetic susceptibility are both very limited. In some senses, we have confirmed that there indeed exists destructive interference within the transparency window, as

predicted by Eq. (3). Meanwhile, it is worth noting slow light in this metamaterial at the transparency window. Figure 4(b) presents the group index (n_g) as a function of frequency in the metamaterial, *i.e.*, $n_g = n + \omega \frac{dn}{d\omega}$, where n is the refractive index of the metamaterial and ω is the frequency of light. As shown in Fig. 4(b), within the frequency regime of the transparent window, the real part of the group index is larger than 1 ($\mathrm{Re}(n_g) \cong 6$), and the imaginary part of the refraction index is very small. It is also worthy to show the figure of merit (FOM) [10] in this metamaterial according to the definition of $FOM = \mathrm{Re}(n)/\mathrm{Im}(n)$, where $\mathrm{Re}(n)$ and $\mathrm{Im}(n)$ are the real and imaginary parts of the refraction index, respectively. It is found that within the frequency regime of the transparent window, the *FOM* of this metamaterial is larger than 10 and the maximum can reach *FOM* =55. This feature agrees well with the retrieved permeability in Fig.3(c), where the imaginary part is almost zero around ω_{EIT}. In some senses, we have achieved a low-loss metamaterial. Therefore, the light can be significantly slowed down and the optical loss is extremely low around ω_{EIT} =191THz. Similar to EIT effect in the atomic system, slow light in this optically magnetic metamaterial has also been verified.

V. An analog of microscopic picture for EIT in a metamaterial and that in an atomic system

In order to understand microscopic process of EIT in present optically magnetic metamaterial, we try to give a direct analog between EIT in a metamaterial and that in an atomic system. Figure 5(a) schematically shows the physical picture for the EIT phenomenon in a three-level system. Suppose that a laser beam (a probe beam) with a frequency of ω_1 is incident onto a three-level atomic system, the energy of the beam would be strongly absorbed and induce a dipole transition from the state |1> to the state |3>. Then an absorption resonance is achieved. If we induce a second laser beam (the drive beam) of frequency ω_2, this drive beam can be absorbed and lead to the dipole transition between the states |2> and |3>. By tuning the probe beam, the electron transitioned from

|1> to |3> may interfere destructively with the electron transitioned from |2> to |3>. Thereafter, theses two dipole transitions are effectively suppressed. This case is equivalent to "generating" an effective state combining both |1> and |2>, and the electronic transition between this effective state and the state |3> is forbidden. Therefore, this effective state is called the "dark state", and the system becomes transparent to the probe beam. That is to say, a narrow transparency window opens on the original absorption profile, and this EIT phenomenon originates from the quantum interference of these two dipole transitions. We can expect that the atom is trapped in a coherent superposition state of |1> and |2>, and the transition between the coherent superposition state and the excited state |3> is dipoled forbidden. Therefore, a transparency window emerges at specific frequency.

Similarly, the EIT-like phenomenon in present metamaterial can be understood based on a V-type three-level system (as schematically shown in Fig. 5(b)). Here, the ground state is considered as the mode without any magnetic fields. When an incident beam shines, the ground state will transition to both the symmetric mode (with lower frequency ω_L) and the antisymmetric mode (with higher frequency ω_H). Between these two frequencies, the state in the structure is a coherent superposition of the symmetric mode and the antisymmetric mode. At specific frequency, these two modes may destructively interfere and effectively form a dark state. The transition from the ground state to the dark state is almost magnetically dipoled forbidden. Thereafter, a transparency window emerges around the specific frequency, and both the real part and the imaginary part of magnetic susceptibility are close to zero, which is expected in Eq. (3).

VI. Summary

In this work, we have theoretically demonstrated that electromagnetic transparency can be induced by optical magnetism in a metamaterial, which is composed of nonmagnetic meta-molecules (without any magnetic elements). Each meta-molecule consists of a SRR as "bright" meta-atom and also a CWP as "dark" meta-atom. It is found that optically

magnetic resonances occur at optical frequencies due to the local magnetic interaction between “bright” meta-atoms and “dark” meta-atoms, thereafter, a transparency window emerges upon the original absorption background. The phenomenon is similar to the EIT in an atomic three-level system, and a microscopic picture is given to compare it with the EIT. Furthermore, low loss and slow light in this metamaterial have also been verified. The investigations may achieve potential applications on integrated optical circuits.

Acknowledgments

This work was supported by the Ministry of Science and Technology of China (Grant Nos. 2012CB921502 and 2010CB630705), the National Science Foundation of China (Grant Nos. 11034005, 61077023, 50972057 and 11021403), and partly by Jiangsu Province (BK2008012) and the Ministry of Education of China (20100091110029). XRH was supported by the U.S. Department of Energy, Office of Science, Office of Basic Energy Sciences, under Contract No.DE-AC02-06CH11357.

References:

[1] V. G. Veslargo, Sov. Phys. Usp. 10, 509 (1968).

[2] J.B. Pendry, A. J. Holden, D. J. Robbins and W. J. Stewart, IEEE Trans. Microwave Theory Tech **47**, 2075 (1999).

[3] D. R. Smith, W. J. Padilla, D. C. Vier, S. C. Nemat-Nasser and S. Schultz, Phys. Rev. Lett. **84**, 4184 (2000); D. Schurig, J. J. Mock, B. J. Justice, S. A. Cummer, J. B. Pendry, A. F. Starr and D. R. Smith, Science **314**, 977 (2006).

[4] Y. M. Liu, X. Zhang, Chem. Soc. Rev. **40**, 2494 (2011).

[5] T. J. Yen, W. J. Padilla, N. Fang, D. C. Vier, D. R. Smith, J. B. Pendry, D. N. Basov, and X. Zhang, Science **303**, 1494 (2004); S. Linden, C. Enkrich, M. Wegener, J. Zhou, T. Koschny, and C. M. Soukoulis, Science **306**, 1351 (2004).

[6] A. N. Grigorenko, A. K. Geim, H. F. Gleeson, Y. Zhang, A. A. Firsov, I. Y. Khrushchev and J. Petrovic, Nature **438**, 335 (2005).

[7] X. Xiong, W. H. Sun, Y. J. Bao, R. W. Peng, Mu Wang, Cheng Sun, X. Lu, J. Shao, Z. F. Li, and N. B. Ming, Phys. Rev. B **80**, 201105R (2009).

[8] J. B. Pendry, Phys. Rev. Lett. **85**, 3966 (2000).

[9] N. Fang, H. Lee, C. Sun, X. Zhang, Science **308**, 534 (2005).

[10] S. Zhang, W. J. Fan, N. C. Panoiu, K. J. Malloy, R. M. Osgood and S. R. J. Brueck, Phys. Rev. Lett. **95**, 137404 (2005).

[11] J. Valentine, S. Zhang, T. Zentgraf, E. Ulin-Avila, D. A. Genov, G. Bartal and X. Zhang, Nature **455**, 376 (2008).

[12] J. B. Pendry, D. Schurig, and D. R. Smith, Science **312**, 1780 (2006); U. Leonhardt, Science **312**, 1777 (2006).

[13] J. Z. Zhao, D. L. Wang, Ru-Wen Peng, Q. Hu, and Mu Wang, Phys. Rev. E **84**, 046607 (2011).

[14] S. Zhang, D. A. Genov, Y. Wang, M. Liu and X. Zhang, Phys. Rev. Lett. **101**, 047401 (2008).

[15] N. Papasimakis, V. A. Fedotov, N. I. Zheludev and S. L. Prosvirnin, Phys. Rev. Lett. **101**, 253903 (2008).

[16]R. Singh, C. Rockstuhl, F. Lederer, and W. Zhang, Phys. Rev. B **79**, 085111 (2009);

[17] S. Y. Chiam, R. Singh, C. Rockstuhl, F. Lederer, W. L. Zhang and A. A. Bettiol, Phys. Rev. B **80**, 153103 (2009).

[18] C. Y. Chen, I. W. Un, N. H. Tai and T. J. Yen, Opt. Express **17**, 15372 (2009).

[19] J. Zhang, S. Xiao, C. Jeppesen, A. Kristensen and N. A. Mortensen, Opt. Express **18**, 17187 (2010).

[20] N. Liu, L. Langguth, T. Weiss, J. Kastel, M. Fleischhauer, T. Pfau and H. Giessen, Nature Mater. **8**, 758 (2009);

[21] N. Verellen, Y. Sonnefraud, H. Sobhani, F. Hao, V. V. Moshchalkov, P. Van Dorpe, P. Nordlander, and S. A. Maier, Nano Lett. **9**, 1663(2009).

[22] P. Tassin, L. Zhang, T. Koschny, E.N. Economou and C.M. Soukoulis, Phys. Rev. Lett. **102**, 053901 (2009).

[23] Y. Lu, H. Xu, J.Y. Rhee, W.H. Jang, B.S. Ham and Y. Lee, Phys. Rev. B **82**, 195112 (2010).

[24] J. Kim, R. Soref and W.R. Buchwald, Opt. Express **18**, 17997 (2010).

[25] P. Tassin, L. Zhang, R. Zhao, A. Jain, T. Koschny, and C. M. Soukoulis, Phys. Rev. Lett. **109**, 187401 (2012).

[26] L. V. Hau, S. E. Harris, Z. Dutton and C. H. Behroozi, Nature **397**, 594 (1999).

[27] D. R. Smith, S. Schultz, P. Markos, and C. M. Soukoulis, Phys. Rev. B **65**, 195104 (2002).

Figure captions:

1. (a) A schematic SRR, which is used as an optically-magnetic bright meta-atom. **(b)** A schematic CWP, which is used as an optically-magnetic dark meta-atom. **(c)** The calculated local electric field (red curve) and magnetic field (black curve) amplitudes versus frequency in the center of the SRR, where the geometric parameters are set as $a=0.5\mu m$, $b=0.1\mu m$, $c=0.04\mu m$, $d=0.075\mu m$, and $t=0.05\mu m$, respectively. There exists a magnetic resonance around ω_0=192THz. **(d)** The calculated local electric field (red curve) and magnetic field (black curve) amplitudes versus frequency in the center of the CWP, where the geometric parameters are set as $u=0.46\mu m$, $v=0.075\mu m$, and $w=0.5\mu m$, respectively. An extremely weak magnetic resonance is around ω_0=192THz.

2. (a) The schematic optically-magnetic meta-molecule, which contains a bright meta-atom (SRR) and a dark meta-atom (CWP). The separation of two meta-atoms is $g = 0.2\mu m$, and the other geometric parameters are given in Fig.1. **(b)**The calculated magnetic field amplitude in the center of the system as a function of frequency. Both the symmetric mode (ω_-) and the antisymmetric mode (ω_+) are found. And the spatial distributions of the magnetic fields in the meta-molecule at different modes: **(c)** ω_-=178THz and **(d)** ω_+ =205THz, respectively.

3. (a) The schematic optically-magnetic metamaterial, where the lattice parameter is $p=1\mu m$, and the other geometric parameters are given in Fig.1. **(b)** The transmission coefficients of the metamaterial as a function of frequency. Two transmission dips are observed at ω_L and ω_H, respectively. And a transmission window appears around $\omega_{EIT}\cong$191THz. **(c)** The retrieved permeability as a function of frequency in the metamaterial. And the spatial distributions of the magnetic fields in the metamaterial at different frequencies: **(d)** $\omega=\omega_L$, **(e)** $\omega=\omega_H$, and **(f)** $\omega=\omega_{EIT}$, respectively.

4. (a) The magnetic susceptibility versus frequency in the metamaterial. **(b)** The real part of the group index (n_g) and the imaginary part of the index of refraction ($Im(n)$) as a function of frequency.

5. The physical pictures of EIT phenomenon are schematically illustrated **(a)** in a

three-level atomic system and **(b)** in present metamaterial, respectively.

Figures 1-5 are as following:

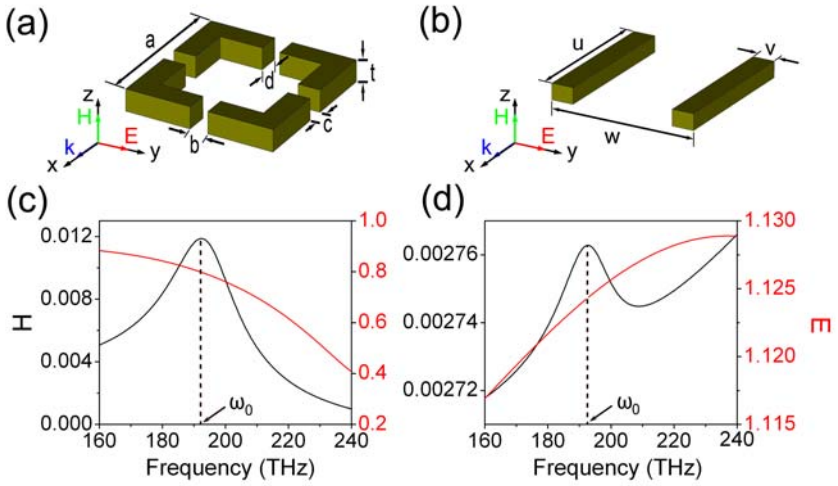

Figure 1 (a) A schematic SRR, which is used as an optically-magnetic bright meta-atom. **(b)** A schematic CWP, which is used as an optically-magnetic dark meta-atom. **(c)** The calculated local electric field (red curve) and magnetic field (black curve) amplitudes versus frequency in the center of the SRR, where the geometric parameters are set as $a=0.5\mu m$, $b=0.1\mu m$, $c=0.04\mu m$, $d=0.075\mu m$, and $t=0.05\mu m$, respectively. There exists a magnetic resonance around ω_0=192THz. **(d)** The calculated local electric field (red curve) and magnetic field (black curve) amplitudes versus frequency in the center of the CWP, where the geometric parameters are set as $u=0.46\mu m$, $v=0.075\mu m$, and $w=0.5\mu m$, respectively. An extremely weak magnetic resonance is around ω_0=192THz.

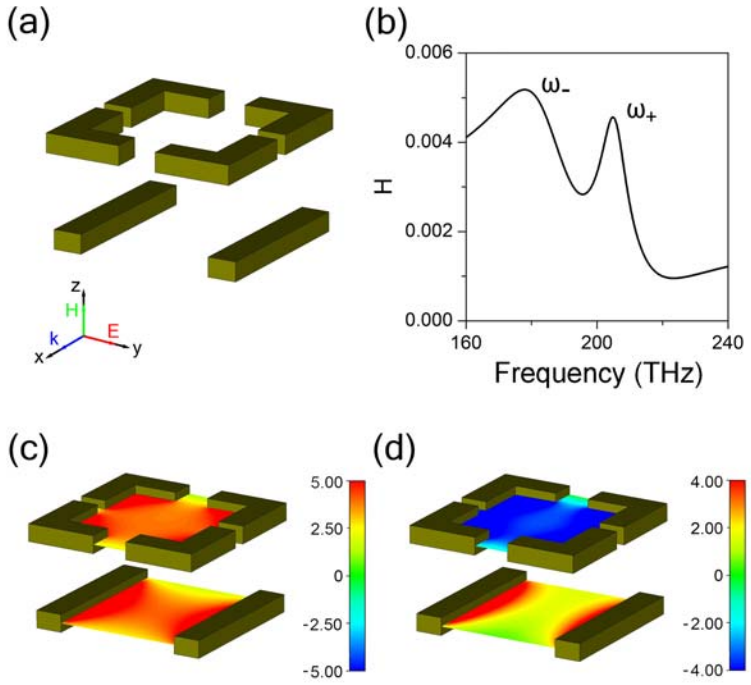

Figure 2 (a) The schematic optically-magnetic meta-molecule, which contains a bright meta-atom (SRR) and a dark meta-atom (CWP). The separation of two meta-atoms is $g = 0.2\mu m$, and the other geometric parameters are given in Fig.1. **(b)** The magnetic field amplitude in the center of the system as a function of frequency. Both the symmetric mode (ω_-) and the antisymmetric mode (ω_+) are found. And the spacial distributions of the magnetic fields in the meta-molecule at different modes: **(c)** ω_-=178THz and **(d)** ω_+ =205THz, respectively.

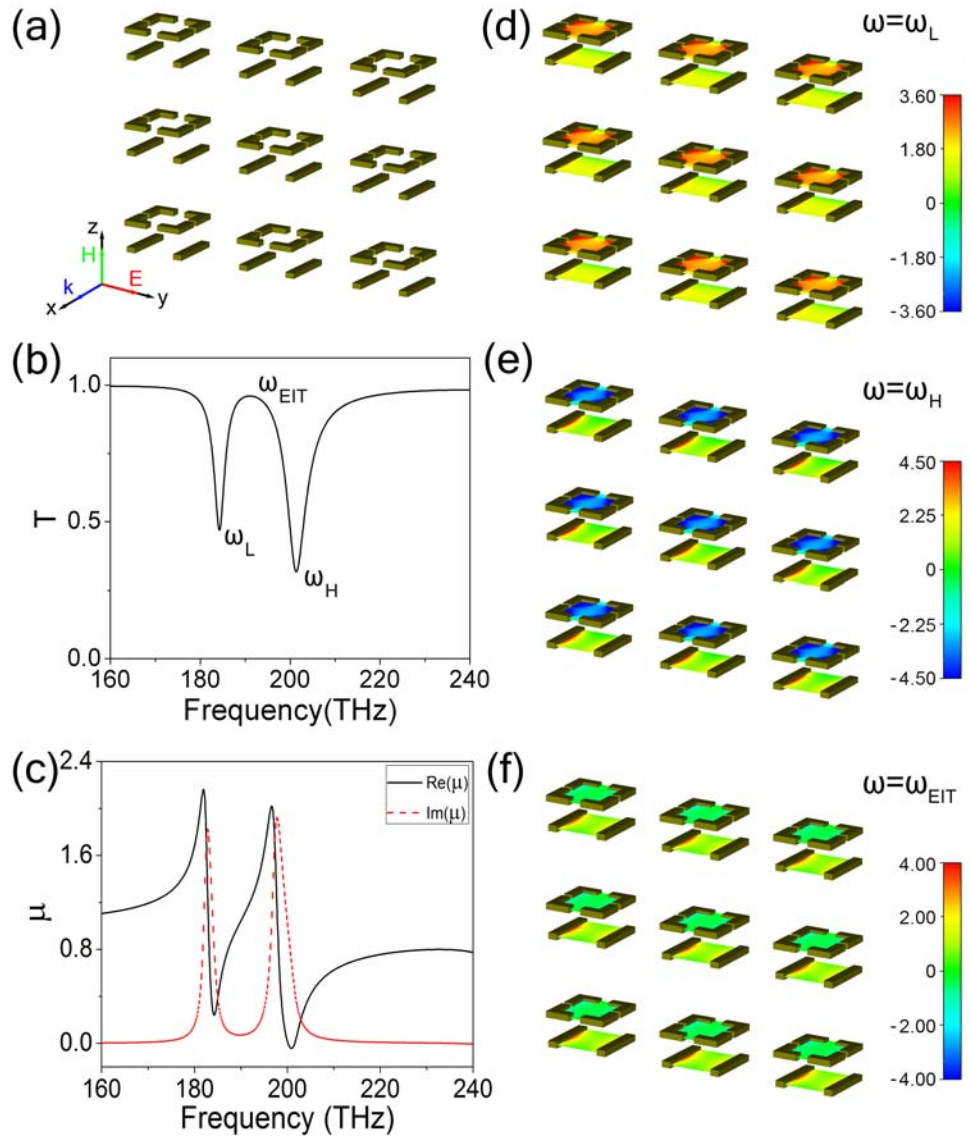

Figure 3 (a) The schematic optically-magnetic metamaterial, where the lattice parameter is $p=1\mu m$, and the other geometric parameters are given in Fig.1. **(b)** The transmission coefficients of the metamaterial as a function of frequency. Two transmission dips are observed at ω_L and ω_H, respectively. And a transmission window appears around ω_{EIT} ≅191THz. **(c)** The retrieved permeability as a function of frequency in the metamaterial. And the spatial distributions of the magnetic fields in the metamaterial at different frequencies: **(d)** $\omega=\omega_L$, **(e)** $\omega=\omega_H$, and **(f)** $\omega=\omega_{EIT}$, respectively.

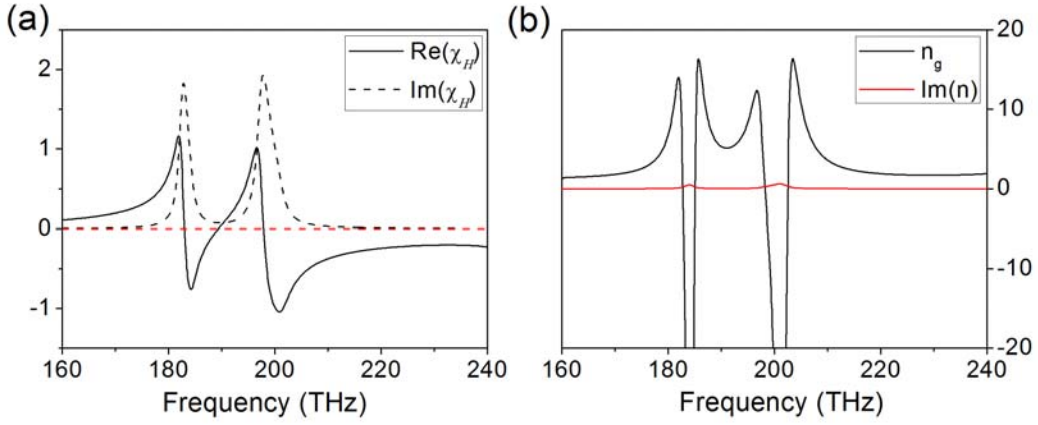

Figure 4 (a) The magnetic susceptibility versus frequency in the metamaterial. **(b)** The real part of the group index (n_g) and the imaginary part of the index of refraction (*Im(n)*) as a function of frequency.

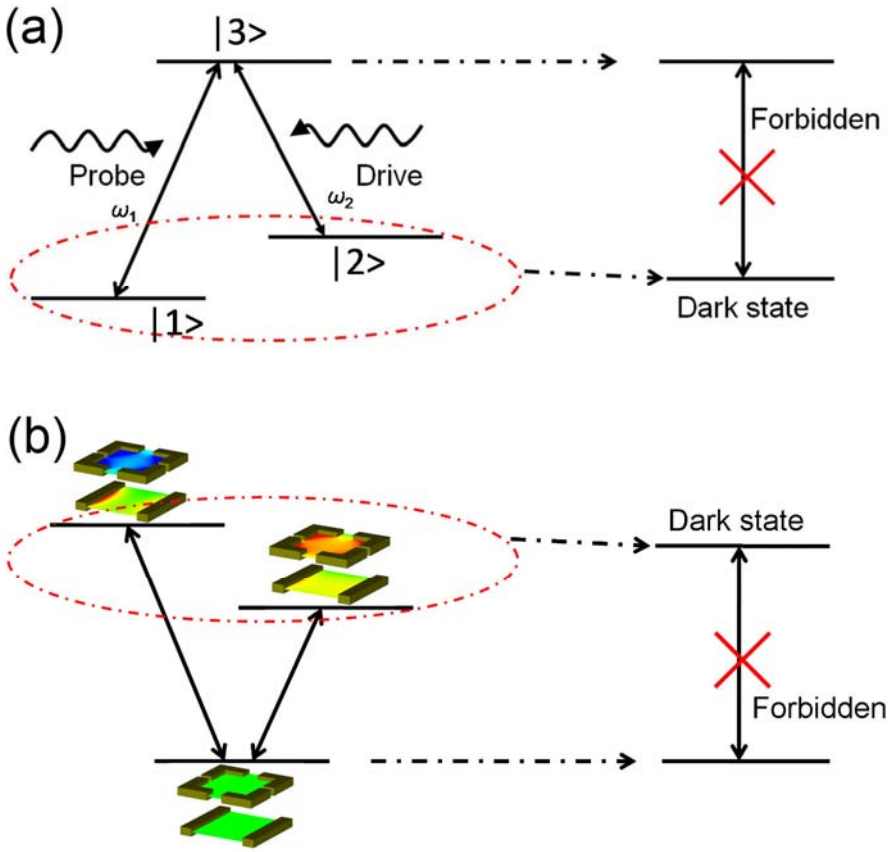

Figure 5 The physical pictures of EIT phenomenon are schematically illustrated **(a)** in a three-level atomic system and **(b)** in present metamaterial, respectively.